BioOne RESEARCH EVOLVED

Computed Tomography of Granulomatous Pneumonia with Oxalosis in an American Alligator (*Alligator mississippiensis*) Associated with *Metarhizium anisopliae* var *anisopliae*

Author(s) :Natalie H. Hall, D.V.M., Kenneth Conley, D.V.M., Clifford Berry, D.V.M., Dipl. A.C.V.R., Lisa Farina, D.V.M., Dipl. A.C.V.P., Lynne Sigler, M.Sc., James F. X. Wellehan, Jr.,D.V.M., Ph.D., Dipl. A.C.Z.M., Dipl. A.C.V.M. (Virology, Bacteriology/Mycology), Michael H. A. Roehrl, M.D., Ph.D., and Darryl Heard, D.V.M., Ph.D., Dipl. A.C.Z.M.
Source: Journal of Zoo and Wildlife Medicine, 42(4):700-708. 2011.
Published By: American Association of Zoo Veterinarians
DOI:
URL: http://www.bioone.org/doi/full/10.1638/2011-0027.1

BioOne (www.bioone.org) is a a nonprofit, online aggregation of core research in the biological, ecological, and environmental sciences. BioOne provides a sustainable online platform for over 170 journals and books published by nonprofit societies, associations, museums, institutions, and presses.

Your use of this PDF, the BioOne Web site, and all posted and associated content indicates your acceptance of BioOne's Terms of Use, available at www.bioone.org/page/terms_of_use.

Usage of BioOne content is strictly limited to personal, educational, and non-commercial use. Commercial inquiries or rights and permissions requests should be directed to the individual publisher as copyright holder.

BioOne sees sustainable scholarly publishing as an inherently collaborative enterprise connecting authors, nonprofit publishers, academic institutions, research libraries, and research funders in the common goal of maximizing access to critical research.

Journal of Zoo and Wildlife Medicine 42(4): 700–708, 2011
Copyright 2011 by American Association of Zoo Veterinarians

COMPUTED TOMOGRAPHY OF GRANULOMATOUS PNEUMONIA WITH OXALOSIS IN AN AMERICAN ALLIGATOR (*ALLIGATOR MISSISSIPPIENSIS*) ASSOCIATED WITH *METARHIZIUM ANISOPLIAE* VAR *ANISOPLIAE*

Natalie H. Hall, D.V.M., Kenneth Conley, D.V.M., Clifford Berry, D.V.M., Dipl. A.C.V.R., Lisa Farina, D.V.M., Dipl. A.C.V.P., Lynne Sigler, M.Sc., James F. X. Wellehan, Jr., D.V.M., Ph.D., Dipl. A.C.Z.M., Dipl. A.C.V.M. (Virology, Bacteriology/Mycology), Michael H. A. Roehrl, M.D., Ph.D., and Darryl Heard, D.V.M., Ph.D., Dipl. A.C.Z.M.

Abstract: An 18-yr-old, male, albino, American alligator (*Alligator mississippiensis*) was evaluated for decreased appetite and abnormal buoyancy. Computed tomography (CT) of the coelomic cavity showed multifocal mineral and soft tissue attenuating pulmonary masses consistent with pulmonary fungal granulomas. Additionally, multifocal areas of generalized, severe emphysema and pulmonary and pleural thickening were identified. The alligator was euthanized and necropsy revealed severe fungal pneumonia associated with oxalosis. *Metarhizium anisopliae* var. *anisopliae* was cultured from lung tissue and exhibited oxalate crystal formation in vitro. Crystals were identified as calcium oxalate monohydrate by X-ray powder defractometry. Fungal identification was based on morphology, including tissue sporulation, and DNA sequence analysis. This organism is typically thought of as an entomopathogen. Clinical signs of fungal pneumonia in nonavian reptiles are often inapparent until the disease is at an advanced stage, making antemortem diagnosis challenging. This case demonstrates the value of CT for pulmonary assessment and diagnosis of fungal pneumonia in the American alligator. Fungal infection with associated oxalosis should not be presumed to be aspergillosis.

Key words: Alligator, *Alligator mississippiensis*, computed tomography, fungal, *Metarhizium*, pneumonia, oxalosis.

CASE REPORT

An 18-yr-old, 2.8-meter, 82-kg, intact male, albino American alligator (*Alligator mississippiensis*) was evaluated at the University of Florida Veterinary Hospitals (Gainesville, Florida, USA) for anorexia and abnormal buoyancy. The alligator was housed alone in an outdoor, 4.3 m × 4.3 m × 1 m, spring-fed, outdoor pool with basking area, which was maintained at a water temperature of 28°C (air temperature range, 8°C to 32°C yearly). The diet consisted of 30 to 40 pellets weekly of Mazuri Crocodilian Large Diet (PMI Nutrition, LLC, St. Louis, Missouri 63144, USA) supplemented with whole-prey items, but the alligator's appetite had decreased over 1 yr to the point of complete anorexia for 1 mo prior to presentation. The animal floated with the left cranial coelom above water level and could submerge only with significant effort. Initial physical examination revealed no additional abnormalities except mild cutaneous abrasions obtained during initial restraint.

The alligator was anesthetized using i.v. propofol (Abbott Laboratories, Abbott Park, Illinois 60064, USA) induction at 1.5 mg/kg in the ventral coccygeal vein, intubated, and then maintained with 1–2% isoflurane (Minrad, Inc., Bethlehem, Pennsylvania 18018, USA) in oxygen. An i.v. catheter was placed in the ventral coccygeal vein for supplemental propofol administration.[39] Computed tomography (CT) of the coelomic cavity was performed with a helical, eight-slice CT scanner (Aquilion 8, Toshiba America Medical Systems, Inc., Tustin, California 92780, USA). Noncontrast volumetric data were acquired using 120 kV, 200 mA, and 0.5 sec/rotation with a pitch of 1, and 5-mm contiguous images were reconstructed using bone and soft tissue algorithms. In addition, 5-mm contiguous dorsal and sagittal reformatted slices were reviewed. CT revealed near complete loss of pulmonary architecture on the right with multifocal areas of suspected

From the Department of Small Animal Clinical Sciences (Hall, Berry, Wellehan, Heard) and the Department of Infectious Diseases and Pathology (Conley, Farina), University of Florida Veterinary Medical Center, 2015 SW 16th Avenue, Gainesville, Florida 32610, USA; the University of Alberta, Microfungus Collection and Herbarium, Devonian Botanic Garden, Edmonton, Alberta T6G 2R3, Canada (Sigler); and the Department of Pathology and Laboratory Medicine, Boston Medical Center, 670 Albany Biosquare III, Boston, Massachusetts 02118, USA (Roehrl). Correspondence should be directed to Dr. Hall (halln@ufl.edu).

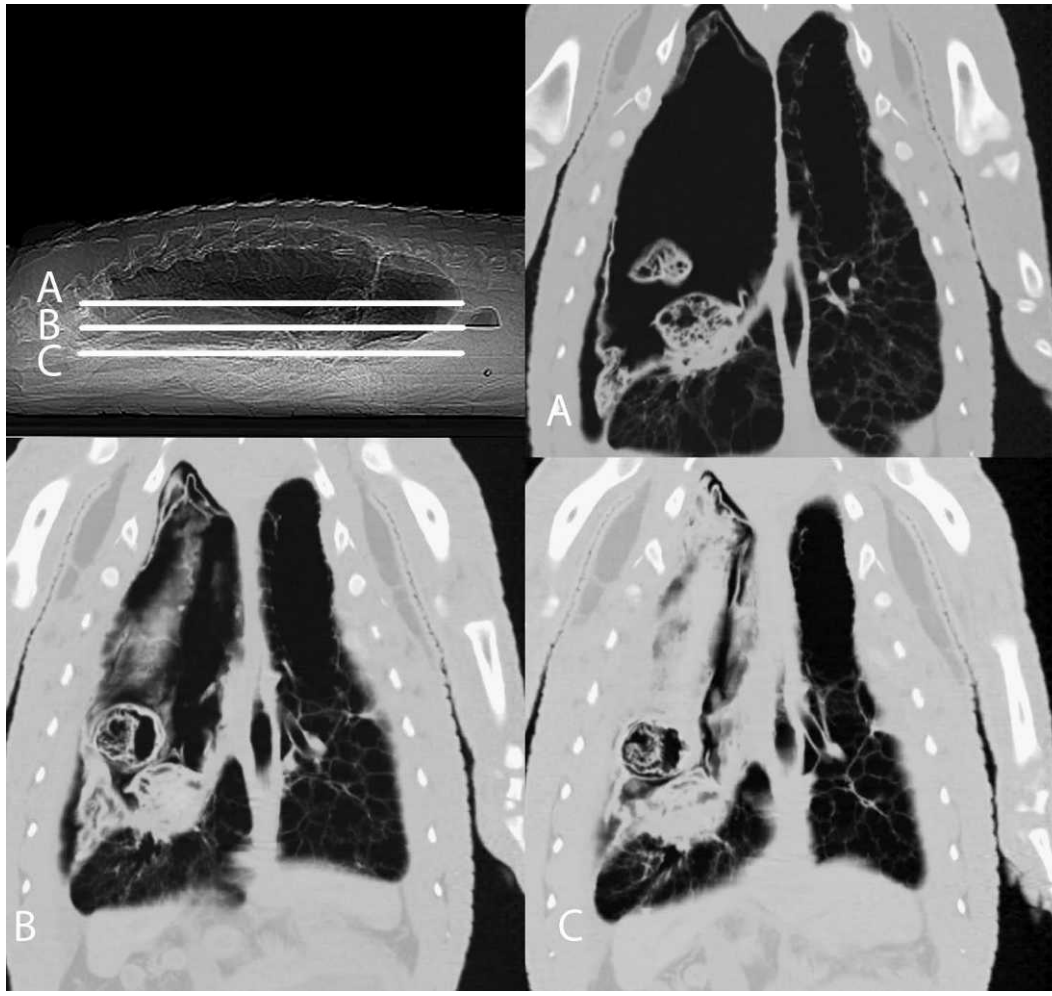

Figure 1. Right lateral scout computed tomography image (upper left) and three dorsal-plane reconstructed images of the thorax. The alligator's head is to the left and dorsal is to the top of scout image. For each of the dorsal-plane images, the right side of the alligator is the viewer's left and the alligator's head is at the top of the image. **A.** Right lung lobe contains large cavitated masses and severe emphysematous changes from cranial to mid-zone region with a small focal pneumocoelom along the right lateral and caudal aspect of the thoracic coelom and thickening of the adjacent portion of right lung lobe. A single, large, curvilinear septation is noted to divide these severe changes from the caudal medial lung segment, where less severe emphysematous changes are present. **B.** Lung image centered on the most severe right-sided pulmonary pathologic changes. Similar changes as seen in Figure 1A are noted. **C.** Left lung has multifocal emphysematous changes (absence of visible lung septation), focal pleural and pulmonary thickening, and mild thickening of the pulmonary septation. All images were reconstructed from 5-mm transverse images and are 5 mm in thickness. A bone algorithm was used for reconstruction. In addition, all images are presented for review with a window width (WW) = 3,500 and a window level (WL) = −350.

atelectasis and a contralateral mediastinal shift toward the left. Free air was suspected in the right lateral and caudal thoracic coelom, although a thin mesothelial membrane may have been present making this air collection intraparenchymal. Multifocal, linear, soft tissue attenuation was identified within the cranial and caudal right lung. Both lungs exhibited multifocal and cavitated masses consistent with fungal granulomas, abscess formation, or neoplasia (Figs. 1–3). Bronchoscopic evaluation was unsuccessful owing to the presence of obstructive debris in the mainstem bronchi and the 100-cm length limitation of the bronchoscope (Storz Veterinary Specialty Fiberscope 6003VB1, Karl Storz Veterinary Endoscopy America, Goleta, California 93117, USA). Be-

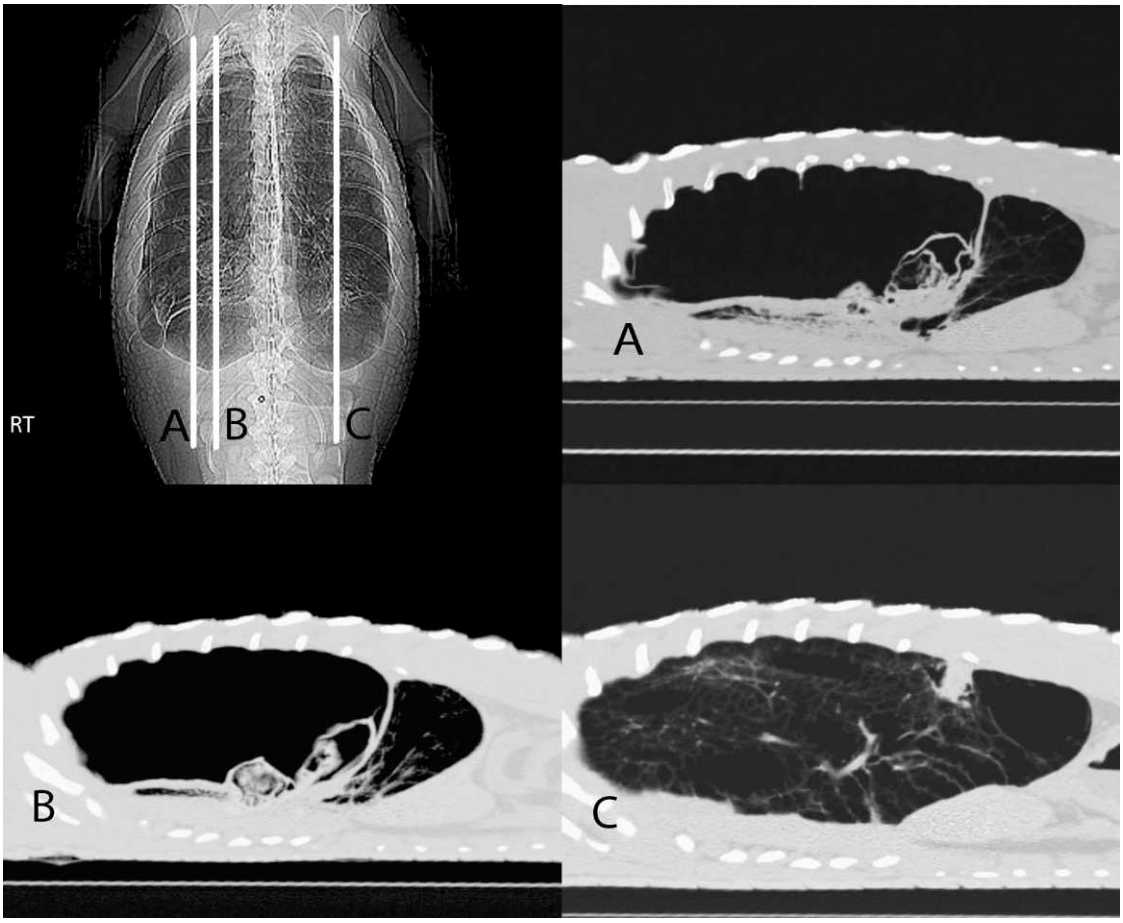

Figure 2. Dorsoventral scout computed tomography image (upper left) and three sagittal plane reconstructed images of the thorax. The alligator's head is at the top, and the alligator's right side is to the viewer's left as marked with the RT (right) in the scout image. The alligator's head is to the left, and dorsal is at the top for each of the sagittal reconstructions. **A.** Right lung lobe with large cavitated mass, ventral plate-like areas of soft tissue thickening of the cranial lung lobe, severe dorsal and cranial emphysema, and marked visceral pleural thickening. **B.** Several right lung lobe cavitated masses with similar changes as seen in Figure 2A. **C.** Left lung with multifocal emphysema (absence of visible lung septation) and focal pleural and pulmonary thickening. All images were reconstructed from 5-mm transverse images and are 5 mm in thickness. A bone algorithm was used for reconstruction. In addition, all images are presented for review with a WW = 3,500 and a WL = −350.

cause of poor prognosis, the animal was euthanized with Beuthanasia-D (Intervet/Schering-Plough Animal Health, 5830 AA Boxmeer, The Netherlands) 0.5 ml/kg i.v. in the supravertebral venous sinus and submitted for necropsy.

Significant gross necropsy findings included bilateral pleural adhesion of the dorsocranial lungs and numerous, variable-sized, multifocal pulmonary granulomas. The left main bronchus was 95% obstructed by green, friable material. Approximately 75% of the right pulmonary lumen was lined by a sheet of tan to green, granular, sturdy, pliable material. Histopathologic examination of this material and the largest pulmonary mass (6.5 cm × 2.5 cm × 1.3 cm) revealed acellular, laminated, eosinophilic material lined by a single layer of multinucleated giant cells and rare heterophils. Numerous shards and aggregates of yellow-tinged, centrally radiating crystals were present within the eosinophilic material. When viewed with polarized light, the crystalline material was birefringent, with a morphologic appearance consistent with calcium oxalate (Fig. 4). Gomori methenamine silver and periodic acid Schiff stains revealed septate, 2- to 5-μm diameter, fungal hyphae associated with the crystals. Staining of other pulmonary masses revealed interwoven septate hyphae of varying widths and

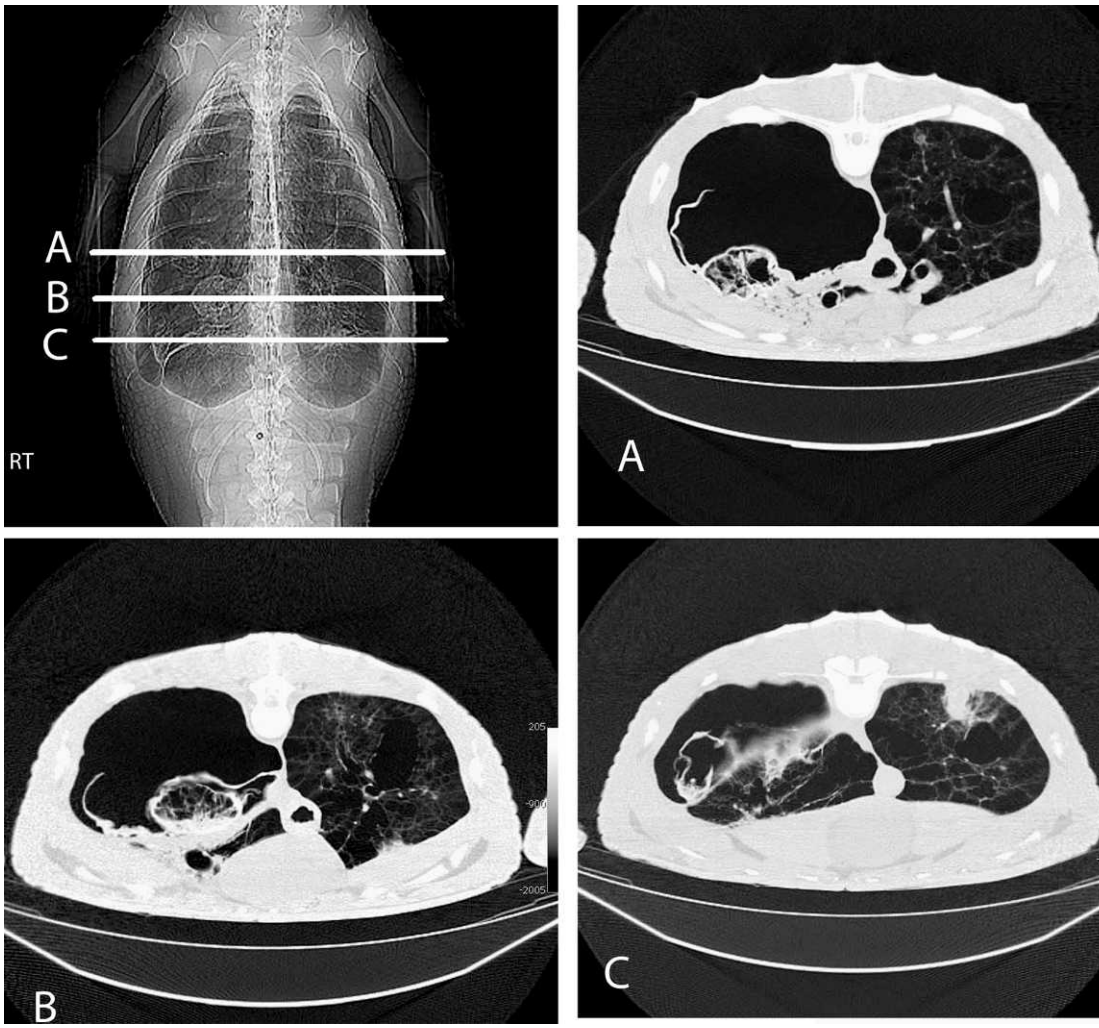

Figure 3. Dorsoventral scout computed tomography image (upper left) and three transverse plane reconstructed images of the thorax. For each of the transverse images shown, the alligator's right is on the viewer's left as marked with the RT (right) in the scout image. **A.** Multifocal severe emphysema in dorsal right lung and, to a lesser extent, in the left lung, and multifocal linear areas of soft tissue attenuation in both lungs. Right lung has multifocal visceral pleural and ventral cavitated masses. **B.** Right lung with the largest fungal granuloma as noted at necropsy. Similar changes as seen in Figure 3A. **C.** Multifocal emphysema (absence of visible lung septation), focal pleural and pulmonary thickening, and a right-side cavitated lesion with a smaller area of focal, round, soft tissue density, consistent with granuloma formation as was seen at necropsy. All images were obtained as 5-mm transverse images. A bone algorithm was used for reconstruction. In addition, all images are presented for review with a WW = 3,500 and a WL = −350.

palisades of cylindrical, pigmented, conidia (ca. 6 μm × 2.5 μm) in chains. The presence of characteristic conidia allowed for the presumptive identification of the fungus as *Metarhizium* species. The intrapulmonary material also contained acellular regions with mixed bacterial aggregates as well as multifocal areas of crystal-associated inflammation and inflammatory debris with few fungal elements.

Fungal culture of pulmonary tissue produced an olivaceous green, fast-growing fungus identified as *Metarhizium anisopliae* based on morphology (cylindrical conidia produced in long, adherent, basipetal chains from branched, subcylindrical phialides). Identification was confirmed as *Metarhizium anisopliae* var. *anisopliae* by internal transcribed spacer (ITS)-2 polymerase chain reaction (PCR) amplification and sequencing of infected

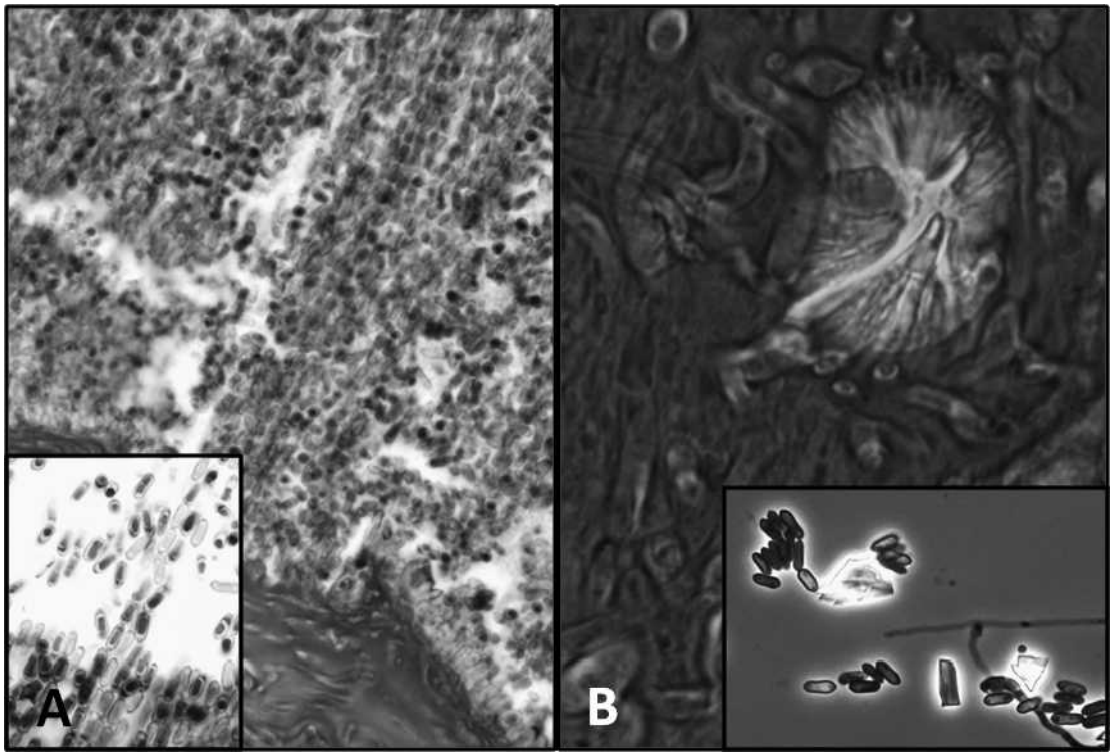

Figure 4. Microscopic features of *M. anisopliae*. **A.** View of the right lung tissue showing adventitious sporulation with characteristic chains of cylindrical conidia. Hematoxylin and eosin (H&E), ×40. Inset is the same tissue at ×100 magnification. **B.** View of the fungal mat within the right lung demonstrating oxalosis with characteristic centrally radiating crystal structure. H&E, ×100. Inset is ×400 magnification of wet mount from cultured isolate exhibiting crystal production and conidiation in vitro.

pulmonary tissue using primers ITS4 and ITS86.[38] Sequence was submitted to GenBank under accession number HQ539658. The isolate was accessioned in the University of Alberta Microfungus Collection and Herbarium as UAMH 11138. The cultured fungal colonies exhibited crystal formation, implicating it as the source of crystals in vivo. Aerobic bacterial culture of pulmonary tissue grew a *Pantoea* species.

The chemical composition of the crystalline deposits was analyzed by X-ray powder defractometry (XRD). The crystals were purified by first clearing lung tissue with 7% (m/v) aqueous sodium hypochlorite at 20°C for 24 to 48 hr. After filtration through a 0.45-μm vacuum-driven filter unit (Merck Millipore, Billerica, Massachusetts 01821, USA), the crystalline residual was washed extensively with water, transferred into a 1.5-ml reaction tube, and dried at 37°C. XRD of an air-dried crystal smear on a glass slide was performed with a Scintag XDS 2000 instrument (Scintag Inc., Cupertino, California 95014, USA) equipped with a 2.2 kW copper K_α X-ray source and a vertical θ-θ goniometer. The most intense d-spacing peaks (2θ angles in parentheses) were observed at 5.91 Å (14.98°), 5.76 Å (15.38°), 3.64 Å (24.46°), 2.96 Å (30.16°), 2.82 Å (31.74°), 2.49 Å (36.02°), 2.35 Å (38.34°), 1.99 Å (45.50°), and 1.98 Å (45.88°). The corresponding d-spacing diffraction peaks of a crystalline calcium oxalate monohydrate standard (monoclinic P21/n space group), as listed in the International Centre for Diffraction Data PDF database (http://www.icdd.com; entry 00-020-0231), are expected to appear at 5.93 Å, 5.79 Å, 3.65 Å, 2.97 Å, 2.84 Å, 2.49 Å, 2.36 Å, 2.00 Å, and 1.98 Å. Based on excellent agreement between the experimentally determined d-spacing values and the database entries, as well as the lack of peaks suggestive of a component of calcium oxalate dihydrate (weddellite) crystals, the crystalline material was identified as calcium oxalate monohydrate ($CaC_2O_4 \bullet H_2O$, whewellite).

DISCUSSION

The chronic anorexia and abnormal buoyancy in this alligator was caused by severe, chronic,

emphysematous and granulomatous pneumonia and pulmonary oxalosis associated with the fungus *Metarhizium anisopliae* var. *anisopliae*. Although bacteria were seen histologically, the distribution was limited to necrotic material within the lung. *Pantoea* spp., which has been reported in healthy reptiles, was isolated by culture. These findings likely represent a secondary bacterial infection of compromised tissue.[10,17,18]

Respiratory mycosis in crocodilians is often associated with opportunistic saprophytic fungi and immunocompromise due to other primary causes.[31] Signs of respiratory mycosis may include increased dyspnea, nasal discharge, and, in aquatic species, alterations in buoyancy.[31] Since clinical signs are often inapparent until advanced disease, antemortem diagnosis of pulmonary mycosis is challenging.[31] Cytologic or histologic demonstration of fungal elements in lung washes, tissue sections, or biopsies is necessary to confirm a fungal etiology.[15,31] Further diagnostics, such as culture and PCR techniques, are then indicated for fungal identification.[15,31] Obtaining a sample of diseased tissue is essential for diagnosis. Lung washes are valuable but may potentially miss areas of abnormal tissue.[15] Similarly, bronchoscopic examination with biopsy, which has the advantage of visualization of the lower respiratory tract, should be guided towards pulmonary lesions to obtain optimal results.[15,20] Therefore, sample collection is best performed when guided by pulmonary imaging to ensure the diseased area of tissue is targeted and appropriately sampled.

Pulmonary imaging in reptiles has traditionally been performed using radiography. Radiographic examinations, however, are compromised by superimposed skeletal structures, soft tissues, and scales.[14] In addition, pulmonary radiographs of crocodilians are compromised by osteoderms, and often, large physical size. CT, an alternative method for lung imaging, is an X-ray based system that allows noninvasive cross-sectional imaging.[14] When compared with thoracic radiography, CT has superior density discrimination and is not complicated by superimposition of overlapping thoracic structures.[32] These advantages have made CT generally accepted as the most reliable imaging technique for detection of pulmonary lesions.[32] CT has been shown to be significantly more sensitive than thoracic radiology in detecting pulmonary soft-tissue nodules in dogs.[26] Reported applications of CT to nonavian reptiles are limited, but include assessment of chelonian skeletal injuries and postmortem assessment of bone density in American alligators.[1,21] This case demonstrates that CT is an effective technique for pulmonary imaging in the American alligator and is useful for antemortem diagnosis of an emphysematous, granulomatous, cavitated pneumonia caused by a primary fungal pathogen.

Fungal pneumonia is not extensively documented in crocodilians and much of the available information consists of reviews and conference proceedings.[31] Reported infections in crocodilians include *Fusarium*, *Mucor*, *Candida*, and *Acremonium* (formerly *Cephalosporium*) species.[5,15,33,37] Fungal pneumonia due to infection with *Aspergillus fumigatus*, *Aspergillus ustus*, and *Fusarium verticillioides* (formerly *F. moniliforme*), as well as with *Beauveria bassiana* in a fatal case with pulmonary fungal mat formation has been reported specifically in the American alligator.[11,13,31] There is one previously reported case in an alligator associating a pneumonia with fungi morphologically consistent with *M. anisopliae*.[3]

Metarhizium anisopliae is rarely identified as a cause of disease in vertebrate species. Few reports exist in the human literature of *M. anisopliae* infection, including sclerokeratitis, sinusitis in immunocompetent humans, and disseminated infection with cutaneous, pulmonary, and cerebral lesions in an immunocompromised child.[2,6,7,16,23,28] In the veterinary literature, spontaneous infection with *M. anisopliae* includes one report of rhinitis in a cat and the previously mentioned report of fungal pneumonia in an alligator.[3,24] *Metarhizium anisopliae* is common in forest and cultivated soils, grows optimally at 25°C, and is considered an entomopathogenic species.[6,35] It infects and kills the larvae of many insect species, including some malaria-vector mosquitoes, and has been used for biocontrol (as has *Beauveria bassiana*).[6,29,35] The *M. anisopliae* complex includes four varieties. The varieties share high sequence homology, which has provided support for their elevation to species status.[4] Recent work has shown that morphologic-based *M. anisopliae* identification to the subspecies level is not reliable, and sequence-based techniques are preferable.[9] Sequence data have also shown that *Metarhizium* has sexual stages (teleomorphs) in the recently described genus, *Metacordyceps*, not *Cordyceps* as previously supposed.[22,36]

The present case exhibits two features not previously reported with *Metarhizium* spp. infection that are uncommon in medical mycology. The first is the presence of reproductive propagules (conidia) in vivo, known as adventitious sporula-

tion, which is valuable for preliminary identification of the organism in tissue. Adventitious sporulation has been associated with *Aspergillus*, *Fusarium*, *Acremonium*, and *Paecilomyces* species and is thought to increase the likelihood of systemic dissemination, improving the chance of a positive blood culture.[11,30] In this case, the presence of conidia in the pulmonary lumen augmented the marked dissemination of *M. anisopliae* throughout the lung and allowed for presumptive identification of the fungus before completion of culture and molecular work. In a live patient, the presence of adventitious sporulation in a surgical biopsy would permit earlier and more specific medical intervention.

The second previously unreported feature of *M. anisopliae*–associated disease is oxalosis in animal tissues. The pulmonary oxalosis reflects the growing conditions in which the *M. anisopliae* was thriving and appears to have contributed to the severity of the disease in this animal by enhancing inflammation and necrosis. Metarhizium anisopliae and other fungi regulate genomic expression to ensure that cell products that function extracellularly are synthesized only at environmental pH levels at which they are effective.[8,34] They may also modify environmental pH by production of bases and acids, such as oxalic acid.[35] In host tissues, the oxalic acid combines with calcium to produce calcium oxalate crystals, which are deposited in adjacent tissues and in debris between the fungal mycelium and the host tissue.[25] Pulmonary oxalosis contributes to severe inflammatory responses, including tissue damage, necrosis, and localized vascular thromboembolism.[19] Pulmonary oxalosis has been well reported in association with *Aspergillus* spp. in humans.[19] Because *Aspergillus* species are by far the most common fungi causing oxalosis in human mycoses, fungal oxalosis is often presumptively considered to be aspergillosis.[27] In veterinary literature, fungal oxalosis has been associated with *Aspergillus niger* in a great horned owl (*Bubo virginianus*) and in an alpaca (*Lama pacos*).[25,40] Similarly to this case of infection with the entomopathogen *M. anisopliae*, the three reported American alligators with fatal infection by the entomopathogenic fungus *Beauveria bassiana* also exhibited pulmonary oxalosis and adventitious sporulation.[12,13] Further investigation may reveal these features to be unique to entomopathogens in crocodilians and helpful in identifying fungal species when additional diagnostic assays are lacking.

CONCLUSION

In conclusion, this case demonstrates the value of computed tomography in crocodilian species for antemortem assessment of severe pulmonary pathology including generalized emphysematous changes and cavitated granuloma formation. Providing high levels of tissue detail free of artifact from superimposed tissues, this diagnostic modality is effective for pulmonary evaluation even in large crocodilians. Using CT, fungal pneumonia was suspected in this patient and confirmed on necropsy. Necropsy findings indicated that *M. anisopliae* var. *anisopliae* can occur as a primary source of infection and oxalosis in the pulmonary tissue of the American alligator. Mycoses in poikilotherms are often associated with species uncommonly seen in mammals, and fungal oxalosis should not be presumed to be aspergillosis.

Acknowledgments: The authors are grateful to William J. Croft, Ph.D., Department of Chemistry and Chemical Biology, Harvard University, and Julia Y. Wang, Ph.D., Channing Laboratory, Brigham and Women's Hospital and Harvard Medical School, for their work in chemical analysis of the calcium oxalate. The authors also thank April Childress, Department of Small Animal Clinical Sciences, University of Florida Veterinary Medical Center, for her valuable assistance in DNA sequence analysis.

LITERATURE CITED

1. Abou-Madi, N., P. V. Scrivani, G. V. Kollias, and S. M. Hernandez-Divers. 2004. Diagnosis of skeletal injuries in chelonians using computed tomography. J. Zoo Wildl. Med. 35: 226–231.

2. Amiel, H., A. B. Chohan, G. R. Snibson, and R. Vajpayee. 2008. Atypical fungal sclerokeratitis. Cornea 27: 382–383.

3. Austwick, P. K. C., and I. F. Keymer. 1981. Fungi and actinomycetes. *In:* Cooper, J. E., and O. Jackson (eds.). Diseases of the Reptilian, vol 1. Academic Press, London, United Kingdom. Pp. 193–231.

4. Bischoff, J. F., S. A. Rehner, and R. A. Humber. 2009. A multilocus phylogeny of the *Metarhizium anisopliae* lineage. Mycologia 101: 512–530.

5. Buenviaje, G. N., P. W. Ladds, L. Melville, and S. C. Manolis. 1994. Disease-husbandry associations in farmed crocodiles in Queensland and the Northern Territory. Aust. Vet. J. 71: 165–173.

6. Burgner, D., G. Eagles, M. Burgess, P. Procopis, M. Rogers, D. Muir, R. Pritchard, A. Hocking, and M. Priest. 1998. Disseminated invasive infection due to

Metarrhizium anisopliae in an immunocompromised child. J. Clin. Microbiol. 36: 1146–1150.

7. De Garcia, M. C., M. L. Arboleda, F. Barraquer, and E. Grose. 1997. Fungal keratitis caused by *Metarhizium anisopliae* var. *anisopliae*. J. Med. Vet. Mycol. 35: 361–363.

8. Dutton, M. V., and C. S. Evans. 1996. Oxalate production by fungi: its role in pathogenicity and ecology in the soil environment. Can. J. Microbiol. 42: 881–895.

9. Fernandes, E. K. K., C. A. Keyser, J. P. Chong, D. E. N. Rangel, M. P. Miller, and D. W. Roberts. 2009. Characterization of *Metarhizium* species and varieties based on molecular analysis, heat tolerance, and cold activity. J. Appl. Microbiol. 108: 115–128.

10. Foti, M., C. Giacopello, T. Bottari, V. Fisichella, D. Rinaldo, and C. Mammina. 2009. Antibiotic resistance of gram negative isolates from loggerhead sea turtles (*Caretta caretta*) in the central Mediterranean sea. Mar. Pollut. Bull. 58: 1363–1366.

11. Freiler, P. F., L. Sigler, and P. E. Nelson. 1985. Mycotic pneumonia caused by *Fusarium moniliforme* in an alligator. Sabouraudia: J. Med. Vet. Mycol. 23: 399–402.

12. Fromtling, R. A., J. M. Jensen, B. E. Robinson, and G. S. Bulmer. 1979. Fatal mycotic pulmonary disease of captive American alligators. Vet. Pathol. 16: 428–431.

13. Fromtling, R. A., S. D. Kosanke, J. M. Jensen, and G. S. Bulmer. 1979. Fatal *Beauveria bassiana* infection in a captive American alligator. J. Am. Vet. Med. Assoc. 175: 934–936.

14. Gumpenberger, M., and W. Henninger. 2001. Use of computed tomography in avian and reptile medicine. Sem. Avian Exot. Pet Med. 10: 174–180.

15. Jacobson, E. R., J. L. Cheatwood, and L. K. Maxwell. 2000. Mycotic diseases of reptiles. Sem. Avian Exot. Pet Med. 9: 94–101.

16. Jani, B. R., M. G. Rinaldi, and W. J. Reinhart. 2001. An unusual case of fungal keratitis: *Metarrhizium anisopliae*. Cornea 20: 765–768.

17. Johnston, M. A., D. E. Porter, G. I. Scott, W. E. Rhodes, and L. F. Webster. 2010. Isolation of faecal coliform bacteria from the American alligator (*Alligator mississippiensis*). J. Appl. Microbiol. 108: 965–973.

18. Joyner, P. H., J. D. Brown, S. Holladay, and J. M. Sleeman. 2006. Characterization of the bacterial microflora of the tympanic cavity of eastern box turtles with and without aural abscesses. J. Wildl. Dis. 42: 859–864.

19. Kradin, R. L., and E. Mark. 2008. The pathology of pulmonary disorders due to *Aspergillus* spp. Arch. Pathol. Lab. Med. 132: 606–614.

20. Lafortune, M., T. Gobel, E. Jacobson, D. Heard, D. Brown, R. Alleman, K. Vliet, K. Harr, and J. Hernandez. 2005. Respiratory bronchoscopy of subadult American alligators (*Alligator mississippiensis*) and tracheal wash evaluation. J. Zoo Wildl. Med. 36: 12–20.

21. Lind, P. M., M. R. Milnes, R. Lundberg, D. Bermudez, J. Orberg, and L. J. Guillette, Jr. 2004. Abnormal bone composition in female juvenile American alligators from a pesticide polluted lake. Environ. Health Perspect. 112: 359–362.

22. Liu, Z. Y., Z. Q. Liang, A. Y. Liu, Y. J. Yao, K. D. Hyde, and Z. N. Yu. 2002. Molecular evidence for teleomorph-anamorph connections in *Cordyceps* based on ITS-5,8S rDNA sequences. Mycol. Res. 106: 1100–1108.

23. Marsh, R. A., A. W. Lucky, T. J. Walsh, M. C. Pacheco, M. G. Rinaldi, E. Mailler-Savage, A. Puel, J. L. Casanova, J. J. Bleesing, M. D. Filippi, D. A. Williams, M. O. Daines, and A. H. Filopovich. 2008. Cutaneous infection with *Metarhizium anisopliae* in a patient with hypohidrotic ectodermal dysplasia and immune deficiency. Pediatr. Infect. Dis. J. 27: 283–284.

24. Muir, D., P. Martin, K. Kendall, and R. Malik. 1998. Invasive hyphomycotic rhinitis in a cat due to *Metarhizium anisopliae*. Med. Mycol. 36: 51–54.

25. Muntz, F. H. A. 1999. Oxalate-producing pulmonary aspergillosis in an alpaca. Vet. Pathol. 36: 631–632.

26. Nemanic, S., C. A. London, and E. R. Wisner. 2006. Comparison of thoracic radiographs and single breath-hold helical CT for detection of pulmonary nodules in dogs with metastatic neoplasia. J. Vet. Intern. Med. 20: 508–515.

27. Pabuççuoğlu, U. 2005. Aspects of oxalosis associated with aspergillosis in pathology specimens. Pathol. Res. Pract. 201: 363–368.

28. Revankar, S. G., D. A. Sutton, S. E. Sanche, J. Rao, M. Zervos, F. Dashti, and M. G. Rinaldi. 1999. *Metarrhizium anisopliae* as a cause of sinusitis in immunocompetent hosts. J. Clin. Microbiol. 37: 195–198.

29. Robert, A., and K. Messing-Al-Aidroos. 1984. Acid production by *Metarhizium anisopliae*: effects on virulence against mosquitoes and on detection of in vitro amylase, protease, and lipase activity. J. Invertebr. Pathol. 45: 9–15.

30. Schell, W. A. 1995. New aspects of emerging fungal pathogens: a multifaceted challenge. Clin. Lab. Med. 15: 365–387.

31. Schumacher, J. 2003. Fungal diseases of reptiles. Vet. Clin. North Am. Exot. Anim. Pract. 6: 327–335.

32. Schwarz, L. A., and A. S. Tidwell. 1999. Alternative imaging of the lung. Clin. Tech. Small Anim. Pract. 14: 187–206.

33. Silberman, M. S., J. Blue, and E. Mahaffey. 1977. Phycomycoses resulting in the death of crocodilians in a common pool. Proc. Am. Assoc. Zoo Vet. 1977: 100–102.

34. St. Leger, R. J., L. Joshi, and D. Roberts. 1998. Ambient pH is a major determinant in the expression of cuticle-degrading enzymes and hydrophobin by *Metarhizium anisopliae*. Appl. Environ. Microbiol. 64: 709–713.

35. St. Leger, R. J., J. O. Nelson, and S. E. Screen. 1999. The entomopathogenic fungus *Metarhizium anisopliae* alters ambient pH, allowing extracellular protease production and activity. Microbiology 145: 2691–2699.

36. Sung, G. H., N. L. Hywel-Jones, J. M. Sung, J. J. Juangsaard, B. Shresthra, and J. W. Spatafora. 2007. Phylogenetic classification of *Cordyceps* and the clavicipitaceous fungi. Stud. Mycol. 57: 1–59.

37. Trevino, G. S. 1972. Cephalosporiosis in three caimans. J. Wildl. Dis. 8: 384–388.

38. Turenne, C. Y., S. E. Sanche, D. J. Hoban, J. A. Karlowsky, and A. M. Kabani. 1999. Rapid identification of fungi by using the ITS2 genetic region and an automated fluorescent capillary electrophoresis system. J. Clin. Microbiol. 37: 1846–1851.

39. Wellehan, J. F. X., M. Lafortune, C. Gunkel, E. Rooney-DelPino, D. Heard, and E. Jacobson. 2004. Coccygeal vascular catheterization in lizards and crocodilians. J. Herpetol. Med. Surg. 14: 26–28.

40. Wobeser, G., and J. R. Saunders. 1975. Pulmonary oxalosis in association with *Aspergillus niger* infection in a great horned owl (*Bubo virginianus*). Avian Dis. 19: 388–392.

Received for publication 7 February 2011